ANNALI DI GEOFISICA, VOL. 42, N. 5, October 1999

Seismic response to stress-strain fields in the lithosphere of Sicily

Graziella Barberi ([1]), Domenico Caccamo ([1]), Gaetano De Luca ([2]), Giancarlo Neri ([1]) and Roberto Scarpa ([2])
([1]) *Istituto di Scienze della Terra, Università di Messina, Italy*
([2]) *Dipartimento di Fisica, Università dell'Aquila, Coppito, L'Aquila, Italy*

Abstract
Earthquake locations and fault-plane solutions are investigated in Sicily and the surrounding areas, by using local network data for the period 1988-1995, and a recently proposed 3D model of the local crustal structure. The results were used for local-to-regional scale stress inversion and strain tensor computations, after integration by a set of selected focal mechanisms taken from the literature. The area under study appears to be affected by heterogeneity of seismic deformation and the stress field. The contraction-to-extension transition from west to east on a regional scale can find a reasonable explanation in the framework of current geodynamic models, such as those assuming the activity of two main tectonic sources in the South Italy region, *e.g.*, the Africa-Europe north-south slow convergence and the faster eastward roll-back of a westward-dipping Ionian subducting slab (Cinque *et al.*, 1993). The analysis of low-magnitude (2.5-4.0) earthquakes permitted us to perform an investigation of local-scale strain heterogeneities in this region and to evidence notable changes in the deformation style when processes at different scales are considered.

Key words *stress – strain – lithosphere – Sicily*

1. Introduction

Before the present work, all local-scale seismological investigations in Sicily and surroundings were performed using 1D seismic wave velocity models (see *e.g.*, Caccamo *et al.*, 1996; Neri *et al.*, 1996). For this reason, and in consideration of strong lateral heterogeneity affecting the crust and mantle structure in the region (Morelli *et al.*, 1975; Calcagnile and Panza, 1981; Calcagnile *et al.*, 1982; Scarpa, 1982; Selvaggi and Chiarabba, 1995; Plomerová *et al.*, 1998), the results were proposed as preliminary. A local tomographic inversion of earthquake and artificial explosion data was recently carried out by De Luca *et al.* (1997) and this allows us to proceed now with the first 3D analysis of source locations, fault plane solutions, and stress and strain tensors. Compared to previous investigations, an improved data set is also used, comprising information from local seismic networks for the period 1988-1995. Thus a check of results from 1D investigations, with related tectonic implications, will be possible. Also, local-scale seismic stress and strain information deriving from the present study will be examined jointly with similar data on larger scales (Rebai *et al.*, 1992; Kiratzi, 1994; Caccamo *et al.*, 1996; Albarello *et al.*, 1997; Ciancio *et al.*, 1997), with geological evidence (Ben Avraham and Grasso, 1990, 1991; Ghisetti, 1992), and with DSS structural information (Finetti and Del Ben, 1986), all with the purpose of contributing to current research on tectonic processes in the area under study.

Mailing address: Prof. Giancarlo Neri, Istituto di Scienze della Terra, Università di Messina, Salita Sperone 31, 98166 S. Agata, Messina, Italy; email: geoforum@imeuniv.unime.it

2. Geodynamic features of the study area

The region under investigation (fig. 1) is characterized by a fairly rapid transition from a nearly oceanic crustal structure beneath the Tyrrhenian abyssal plain to a continental-like structure beneath Sicily and Calabria (Morelli *et al.*, 1975; Calcagnile and Panza, 1981; Scarpa, 1982; Calcagnile *et al.*, 1982; Selvaggi and Chiarabba, 1995; Plomerová *et al.*, 1998). Many fault discontinuities have been mapped, on the grounds both of geological and geophysical investigations: i) NW-SE transcurrent fault systems in the Southernmost Tyrrhenian, generating earthquakes with maximum magnitudes up to 5.5 (Frazzetta *et al.*, 1982; Finetti and Del Ben, 1986; Neri *et al.*, 1996); ii) NE-SW graben structures in the Messina Strait and Southern Calabria, responsible for the strongest earthquakes of Italy, with magnitudes around 7 (Martini and Scarpa, 1983; Ghisetti, 1984, 1992); iii) E-W reverse faults in Central and Western Sicily, producing up to magnitude 6 seismic events (Ben Avraham and Grasso, 1990, 1991).

Several, often contrasting, tectonic hypotheses have been proposed for the region, such as active subduction beneath the Southern Tyrrhenian Sea (Barberi *et al.*, 1973), rifting dominated by slab sinking and passive subduction (Finetti and Del Ben, 1986; Patacca *et al.*, 1990; Cinque *et al.*, 1993), growth of mantle diapirs in the whole Tyrrhenian area (Locardi, 1988; Locardi and Nicolich, 1988) and northeastward compression by the African plate (Mantovani *et al.*, 1990). The debate is apparently far from being concluded. Basic aspects, such as the re-

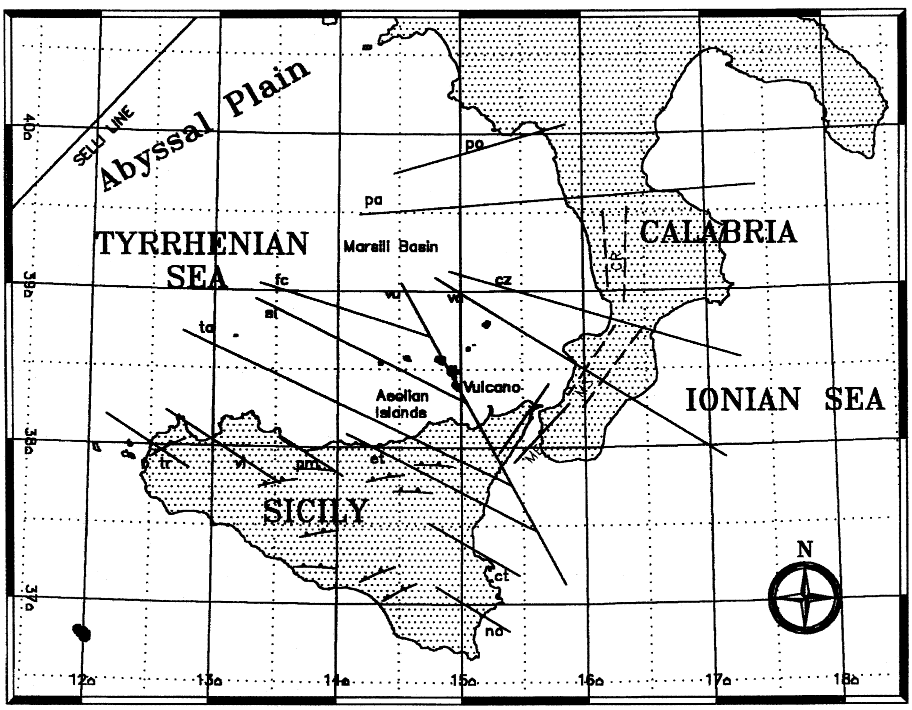

Fig. 1. Map of the study area with locations of the main fault systems: tr = Trapani; no = Noto; vi = S. Vito; pm = Palermo; ct = Catania; et = Etna; ta = Taormina; si = Sisifo; fc = Filicudi; vu = Vulcano; va = Capo Vaticano; cz = Catanzaro; pa = Palinuro; po = Policastro; ME = Messina graben; MS = Mesima graben; CR = Crati graben. (Ghisetti and Vezzani, 1982; Finetti and Del Ben, 1986).

cent evolution of interaction between Africa and Europe (still converging?), are a subject of discussion and disagreement among researchers (*e.g.*, Locardi and Nicolich, 1988; Mantovani *et al.*, 1990; Pollitz, 1991; Albarello *et al.*, 1993; Scandone, 1993; Tamburelli *et al.*, 1993; Mantovani *et al.*, 1997). Enlargement and improvement of data sets is needed to put adequate constraints on this debate. The present study of earthquake and stress-strain patterns in a crucial sector of the Tyrrhenian region like Sicily is intended to make a contribution in this framework.

3. Data and methods of analysis

Local events clearly recorded at a minimum of ten Sicilian stations during the 1988-1995 time interval were selected for reading of *P*- and *S*-wave arrival times, and *P*-onset polarities. First, hypocenter locations were performed by the HYPO71 routine (Lee and Lahr, 1975) in a two-layer, one-dimensional crustal structure (table I) chosen on the grounds of results from previous comparison tests among models (Neri *et al.*, 1991). A standard value of 1.73 was assumed for the V_p/V_s ratio. Then, Thurber's (1983, 1993) 3D location algorithm was applied for hypocentral computations in the laterally varying crustal structure proposed by De Luca *et al.* (1997) for the area under study. As expected, an improvement in locations in terms of seismic wave arrival-time residuals was obtained, in particular an average of 0.44 s was found over the whole data set, clearly lower than the value of 0.64 s coming from 1D locations. Seismic-ray take-off angles derived from the application of HYPO71 and Thurber's algorithms were used for focal mechanism computations (FPFIT code; Reasenberg and Oppenheimer, 1985) in the 1D and 3D structures, respectively. For each event, both the numerical values of fault parameter errors and the stereo-projection of all orientations for *P* and *T* axes compatible with the available polarity data, were taken from the FPFIT output files in order to evaluate the quality both of 1D and 3D solutions. All indicators revealed that 3D solutions are better constrained than 1D ones, so that the former were used to generate the focal mechanism data set for stress inversion and strain tensor computations (table II). Only solutions constrained to 30° were selected, and each of them was assigned a weight (2 or 1) based on its uncertainty (< 20° or in the range 20°-30°, respectively).

Table I. 1D P-wave velocity model used for earthquake locations in the first step of the present investigation. Appropriate station corrections (Neri *et al.*, 1991) were adopted when using this model. Layer velocities (*v*) and upper boundaries (*h*) are expressed in km/s and km (b.s.l.), respectively.

1D velocity model	
$v_1 = 5.57$	$h_1 = 0.0$
$v_2 = 6.50$	$h_2 = 15.0$
$v_3 = 7.76$	$h_3 = 33.0$

Stress inversion was performed by the Gephart and Forsyth (1984) method to estimate the orientations of the main stress axes and the measure *R* of relative stress magnitudes

$$R = (\sigma_2 - \sigma_1)/(\sigma_3 - \sigma_1)$$

under the assumptions that: 1) stress is uniform in the rock volume concerned with the focal mechanisms under investigation; 2) earthquakes are shear dislocation episodes on pre-existing faults, and 3) slip occurs in the direction of the resolved shear stress on the fault plane. A misfit variable is used in the algorithm to define discrepancies between the stress tensor and observations (FPSs): for a given stress model, the misfit of a single focal mechanism is defined as the minimum rotation about any arbitrary axis that brings one of the nodal planes, its slip direction and sense of slip, into an orientation that is consistent with the stress model. The procedure uses a grid-technique operating in the whole space of the stress parameters, and searches for the stress tensor minimizing the average of misfits relative to all FPSs available in the rock volume investigated. The minimum «average misfit» (*F*-value) provides a guide to how well the assumption of stress homogeneity is fulfilled in relation to the seismic sample sub-

Table II. Order number, date, origin time, hypocentral parameters, HYPO71 RMS-value, duration magnitude, FPFIT fault-plane solutions and related errors for all earthquakes analyzed in the present work, excluding those from the literature. *W* is the weight assigned to each FPS according to its constraint level, as evaluated from the FPFIT output files. The number of polarities used for FPS computations is between 8 and 29, with an average of 15.

No.	Date	O.T.	Lat.	Long.	Depth	RMS	Mag	Dip Az	Dip	Rake	D-DA	D-DI	D-RK	*W*
01	880308	0840 13.94	38.367	15.902	039.73	0.43	3.4	210	55	−070	10	03	05	2.0
02	880417	1520 33.02	38.485	14.668	012.73	0.56	2.9	110	30	−180	00	00	00	2.0
03	880605	1243 07.51	38.418	14.673	015.80	0.47	3.7	255	85	0070	13	05	05	2.0
04	880610	0131 42.49	38.193	15.161	009.12	0.38	2.6	210	50	−080	00	00	00	2.0
05	880723	1758 50.26	38.738	15.624	076.36	0.41	3.6	090	70	−070	00	03	10	1.0
06	881007	1622 23.04	38.478	14.655	017.96	0.67	2.6	260	10	0130	05	05	10	1.0
07	881107	1426 54.59	38.108	15.841	019.83	0.28	3.6	225	50	0110	18	00	05	2.0
08	881108	0813 53.56	38.126	15.858	021.56	0.29	2.9	150	65	−030	20	13	15	1.0
09	881211	2356 32.74	37.876	14.983	015.82	0.53	3.1	160	70	−080	05	10	00	2.0
10	890123	0822 54.44	37.864	15.512	021.50	0.41	3.0	250	05	0040	10	03	10	2.0
11	890526	2219 17.59	38.155	15.113	014.92	0.26	3.1	070	50	−170	10	10	10	2.0
12	890619	2122 19.00	37.852	16.188	060.38	0.31	2.7	165	30	−120	08	00	10	2.0
13	890624	0234 18.35	37.845	14.748	012.09	0.52	3.3	135	35	−140	03	08	05	2.0
14	890717	1357 27.62	37.589	16.209	023.72	0.62	2.7	075	10	−130	18	05	35	1.0
15	891105	0226 44.42	38.445	14.936	005.31	0.42	2.5	050	90	−090	00	03	05	2.0
16	900218	0028 46.91	38.101	15.133	020.05	0.32	3.3	175	60	−060	03	10	10	1.0
17	900226	0311 60.06	38.595	14.350	020.02	0.62	3.3	145	65	−140	03	08	00	2.0
18	900328	0547 31.93	38.160	14.908	024.12	0.48	4.2	075	30	−120	08	03	10	2.0
19	900404	1503 38.80	38.245	15.053	015.66	0.50	3.2	125	65	−070	05	10	15	1.0
20	900510	0647 54.92	38.247	15.506	021.50	0.50	3.0	090	55	0110	03	03	10	2.0
21	901005	2305 15.14	37.830	16.144	024.33	0.55	3.0	170	30	−060	13	03	25	1.0
22	901218	1749 39.92	38.138	15.150	013.44	0.32	3.0	120	55	−110	05	05	10	2.0
23	910427	0057 02.01	38.775	15.689	065.83	0.13	3.3	335	85	0060	05	08	05	2.0
24	910518	1008 24.99	38.510	15.435	065.72	0.39	3.1	085	25	0030	03	03	05	2.0
25	910804	0139 40.42	37.784	16.272	025.06	0.67	3.3	120	55	0090	08	05	05	1.0
26	910821	0242 01.27	39.088	15.902	048.97	0.25	3.7	235	10	−080	20	03	25	1.0
27	910906	1559 16.66	39.048	15.552	016.77	0.67	3.3	190	30	0160	00	03	00	2.0
28	910907	0539 19.39	37.984	15.490	013.28	0.25	3.8	115	85	−130	03	03	05	2.0
29	910924	0004 11.14	37.677	14.879	027.70	0.44	3.1	310	50	−060	10	20	10	1.0
30	911003	0240 28.57	38.829	15.206	018.40	0.72	3.8	120	70	0120	05	20	20	1.0
31	950411	1206 52.18	37.602	13.894	027.03	0.40	3.8	240	65	−040	08	08	10	2.0

mitted to inversion (Michael, 1987). In the light of findings from synthetic tests carried out by Wyss *et al.* (1992) to identify the relationship between FPS uncertainties and the F-value in the case of uniform stress, it is assumed in the present study that the condition of a uniform stress tensor is fulfilled if F-values around 3°-4° are obtained, whereas values of the order of 6° and over probably reflect some level of stress heterogeneity. Also, the analysis of earthquake individual misfits with respect to the stress model is performed to define the stress heterogeneity level in the data set. The solution confidence limits estimated according to Parker and McNutt (1980) give additional information because they generally tend to increase for increasing stress heterogeneity. Confidence limits are finally to be considered a reliable *a posteriori* indicator of the FPS data set suitability for stress inversion. More details of the method, and a full description of applications can be found in several papers, such as those by Gephart and Forsyth (1984), Wyss *et al.* (1992) and Gillard *et al.* (1996).

The algorithm used for computing seismic strain parameters and related uncertainties was derived from Kostrov's (1974) method by Wyss *et al.* (1992). The basic data are earthquake magnitudes and fault plane solutions. Magnitude M is converted into scalar moment M_0 by an appropriate relationship, in our case $\log M_0 = 1.5\,M + 16.27$ (Kiratzi, 1994). Other moment-magnitude relationships available in the literature for the study region (*e.g.*, Giardini *et al.*, 1984) proved not to change the results of our strain investigation appreciably. The scalar moment M_0^k of each earthquake is combined with its fault plane solution in order to obtain the moment tensor M_{ij}^k of the event. The moment tensors of all the available events are used for the computation of the strain tensor elements ε_{ij}, after having assigned numerical values to the shear modulus μ and the rock volume V under investigation

$$\varepsilon_{ij} = \frac{1}{2\mu V} \sum_k M_{ij}^k .$$

Values assigned to the shear modulus and volume do not, however, influence the orientation of the principal axes in the strain tensor computation. In the present study, attention is focused on strain orientations; therefore μ and V values adopted for the computations will not be reported. Uncertainties in the computed strain parameters are estimated using a procedure by Wyss *et al.* (1992), based on the use of the covariance matrix formalism, assuming that: 1) there are no systematic errors, and 2) the errors of the scalar moment, strike and dip are independent of each other. How well assumptions (1) and (2) are fulfilled in any specific case is not easy to state, but several tests in previous investigations have shown the general validity of the procedure (Wyss *et al.*, 1992; Gillard *et al.*, 1992; Ciancio *et al.*, 1997). Alternative methods for strain error estimates, based on bootstrap procedures, are under investigation (Albarello *et al.*, 1997).

4. Data from the literature

An accurate evaluation of FPSs reported in the literature was performed for the study region. Fairly restrictive selection-weighting criteria were adopted for inclusion in the data set used for the stress inversion and strain computations. In the papers we examined the polarity distributions in the focal sphere stereographic representations, also trying to evaluate the information available on hypocenter-network relative locations and on the earth structure along the source-station paths. Comparisons have been made among solutions obtained by different authors and methods for the same event. Selected solutions are reported in table III, with a individual weighting factor W (2 or 1), which we assigned following a criterion as compatible as possible with that adopted in the case of solutions computed in the present study (table II, previous section).

5. Discussion of results

Figure 2 shows the epicenter map and two vertical sections of hypocenters, for the earthquakes listed in tables II and III, the fault-plane solutions of which can be considered of quality

Table III. Order number, date, origin time, hypocentral parameters, magnitude and fault-plane solutions of earthquakes selected from the literature (the bibliographic reference is indicated in the last column). *W* is the weight assigned to the FPS (see text), its sign indicates reverse (–) or direct (+) mechanism. Bib: 1 = Dziewonsky *et al.* (1987); 2 = Dziewonsky *et al.* (1991); 3 = Frepoli *et al.* (1993); 4 = Gasparini *et al.* (1985); 5 = Giardini *et al.* (1995); 6 = Anderson and Jackson (1987).

No.	Date	O.T.	Lat.	Long.	Depth	Mag	Az1	Dip1	Az2	Dip2	*W*	Bib
32	081228	0420 –	38.120	15.600	010.00	7.0	208.0	55.0	349.0	42.0	+1.0	4
33	410316	1635 –	38.440	12.120	020.00	6.9	020.0	53.0	217.0	38.0	+1.0	4
34	671031	2108 –	37.840	14.600	038.00	5.0	089.0	61.0	273.0	80.0	+1.0	4
35	680115	0133 –	37.890	13.080	020.00	5.1	040.0	82.0	302.0	46.0	–1.0	4
36	680115	0201 –	37.750	12.980	010.00	5.4	270.0	50.0	156.0	64.0	–1.0	6
37	680116	1642 –	37.860	12.980	036.00	5.1	250.0	58.0	150.0	75.0	–1.0	6
38	680125	0956 –	37.690	12.970	003.00	5.1	270.0	64.0	165.0	62.0	–1.0	6
39	680519	0937 –	38.520	14.820	039.00	4.8	313.0	45.0	198.0	67.0	–1.0	4
40	680616	1303 –	37.780	14.650	023.00	4.8	020.0	80.0	272.0	31.0	–0.0	4
41	760917	0123 –	37.920	14.570	033.00	4.4	322.0	69.0	200.0	36.0	+1.0	4
42	780311	1920 –	38.100	16.030	033.00	5.6	183.0	82.0	255.0	31.0	+1.0	4
43	780415	2333 55.80	38.390	15.070	021.00	5.5	135.0	60.0	043.0	86.0	+2.0	1
44	800528	1951 –	38.480	14.520	012.00	5.7	052.0	62.0	278.0	37.0	–2.0	6
45	901213	0024 34.10	37.250	14.900	015.00	5.4	274.0	64.0	007.0	85.0	–2.0	2-5
46	930728	2128 37.19	37.966	14.167	002.50	3.8	061.0	60.0	205.0	38.0	–1.0	3

suitable for stress inversion and strain computations. The map is not claimed to be representative of the space distribution of activity in the study region, considering the geometry of the network used for the analysis (fig. 2), and the criteria adopted for earthquake selection. Most of data available refer to earthquakes located in Northeastern Sicily, in the Aeolian Islands, and around the Messina Straits. The cluster of four shocks in Western Sicily corresponds to the swarm activity of 1968 in the Belice Valley. Seismicity in the Aeolian area is located in accordance with two fault systems (Sisifo and Vulcano, fig. 1; Finetti and Del Ben, 1986) which have already been identified as major seismogenic structures in the region (Neri *et al.*, 1996). The hypocenters are located at lithospheric depths (fig. 2).

The fault-plane solutions (figs. 3 and 4) reveal a notable variation in the seismic deformation style over the study region, from Western Sicily (dextral strike-slip mechanisms with reverse component; events No. 35 to 38 in table III), to Central Sicily and the Tyrrhenian coast (normal faulting) and the Messina Straits (heterogeneity). The Southern Tyrrhenian area shows some degree of heterogeneity, too, even though both events of magnitude $M > 5$ in this sector (No. 43 and 44 in table III) display a notable compressive component, with P axes oriented nearly N-S.

Strain tensor orientations estimated from several subsets of the whole sample (tables II and III) are reported in fig. 5a-c, together with the 90% confidence limits of the maximum (ε_1) and minimum (ε_3) shortening axes. The subset including all events of magnitude $M > 4$, except for the 1908 Messina Straits event, led to the result given in fig. 5a. The nearly N-S orientation of ε_1 is better constrained than ε_3, which appears practically unconstrained in a roughly E-W vertical plane. This situation can be easily explained in terms of structural heterogeneity of

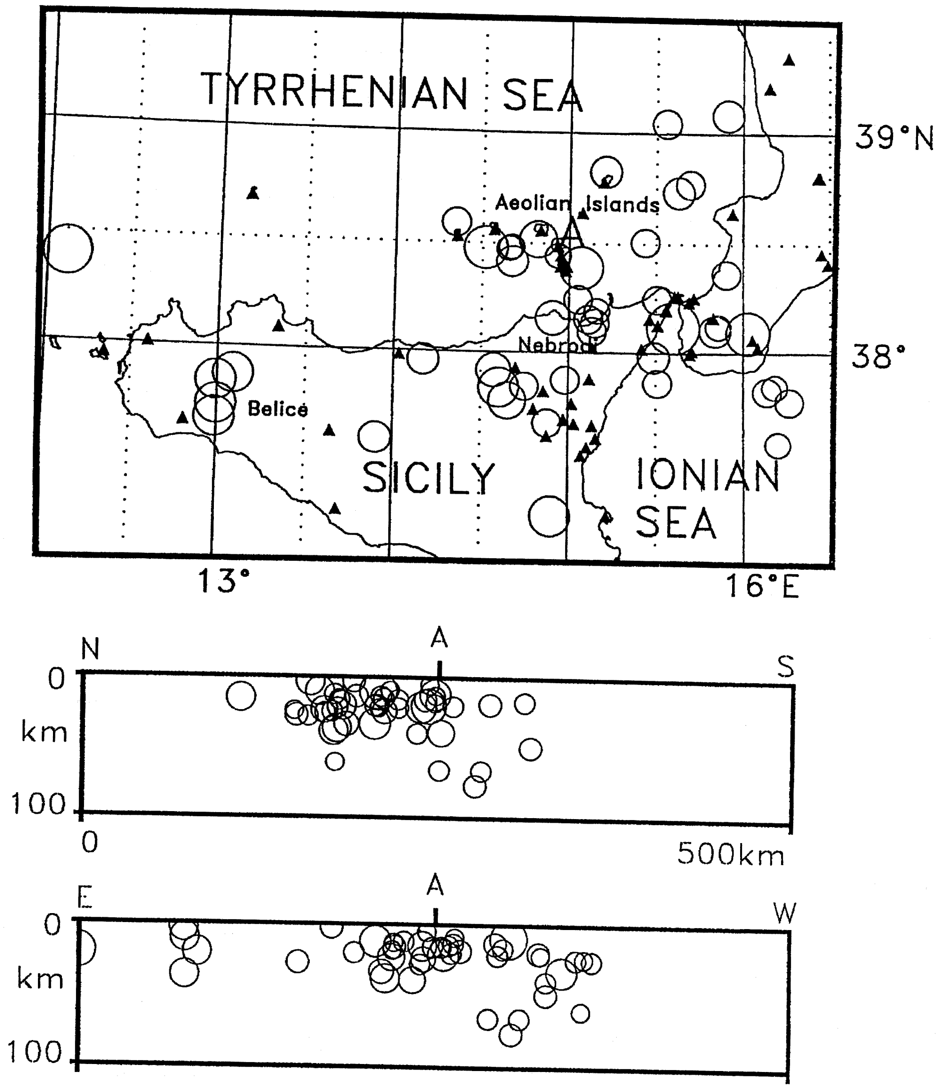

Fig. 2. Epicentral map and hypocenter vertical sections for the earthquakes listed in tables II and III, of which the fault-plane solutions are considered of quality suitable for stress inversion and strain computations. Triangles in the map indicate the locations of seismic stations in the study area.

the study volume. Inclusion of the 1908 normal-faulting event (magnitude 7) led to a radical change in the result (not reported for the sake of conciseness), which means that the event is not compatible with the strain tensor of fig. 5a. There is agreement between the observed seismic strain features and the regional-scale geologic information (fig. 1), showing a transition from a N-S compressive domain in Western and Southern Sicily to a tensional regime in the Calabro-Peloritan arc (Ben Avraham and Grasso, 1990, 1991; Ghisetti, 1992). Results from smaller-

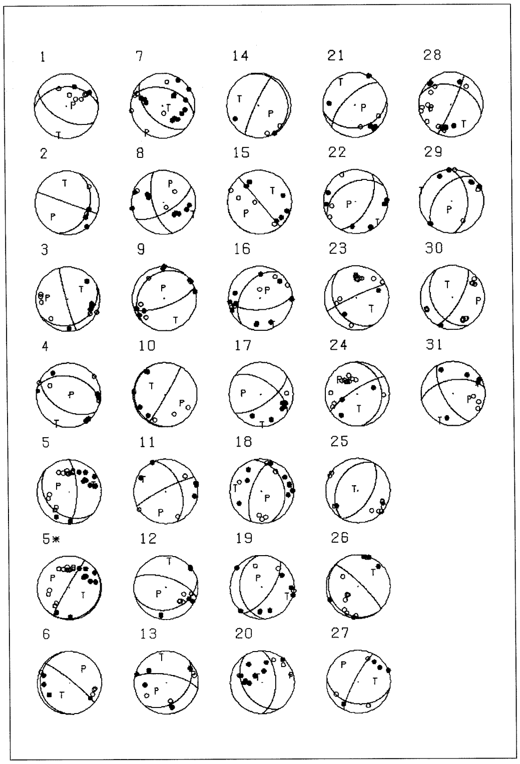

Fig. 3. Fault-plane solutions computed in the present study (lower hemisphere projections). Numerical values are given in table II.

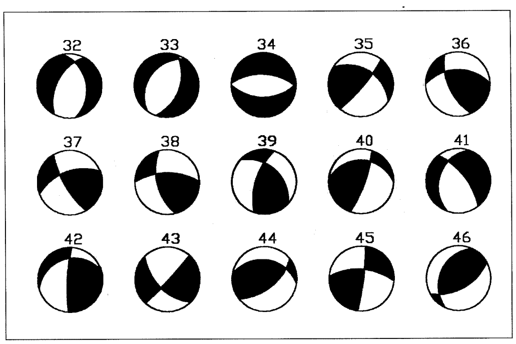

Fig. 4. Fault-plane solutions selected from the literature (lower hemisphere projections). Numerical values and bibliographic references are given in table III.

scale seismic strain analyses are reported in fig. 5b,c. Panel 5b shows that the sector including the Nebrodi chain and the Tyrrhenian coast to the north (for which the maximum magnitude in the data set is 5.0) is characterized by a ε_1 orientation significantly different from that of fig. 5a. It is well known (see *e.g.*, Rebai *et al.*, 1992) that local-scale stress-strain situations may differ from the regional-scale values because of structural heterogeneity. This may account for the results of fig. 5a,b. Further evidence of small-scale strain heterogeneity is given by large confidence areas found by investigation of low-magnitude (< 4.5) events in the Southern Tyrrhenian (fig. 5c).

The most significant results from the stress inversion runs are reported in table IV and fig. 6. First, the entire set of fault-plane solutions was inverted (ALL in table IV): the fairly large value of misfit (F = 11.5°) shows that no uniform stress distribution may explain the whole set of data. Then, several subsets of events were defined corresponding to smaller rock volumes in the study area, some of which are reported in fig. 7. Different magnitude partitions were also used to analyze tectonic processes acting on different scales, according to the principle discussed above. The only data set for which we found an acceptably low value of F (5.1°) is that corresponding to sector $M4$ (fig. 7), with magnitudes M > 4.0. This sector covers most of the study region, the Messina Straits being excluded again. The confidence limits of the stress orientations (fig. 6) reveal an acceptable level of constraint both on σ_1 (low-dip north-south oriented) and σ_3 (nearly east-west). Stress inversion results confirm the findings of the strain analysis. If the magnitude threshold is reduced from 4.0 to 3.5 in the data set relative to the whole study area (ALL4 and ALL35 in table IV) the F-value rises from 6.4° to 9.0°, indicating a clear increase of stress heterogeneity when smaller scale processes are involved. Finally, notable stress heterogeneity was proved to exist also in subvolumes of the study region (WEST, TYR, AEOL and EAST, fig. 7 and table IV) by an analysis of events of every magnitude (M > 2.5). Magnitude partitions were not possible in this specific analysis because of the limited number of data available in each subvolume.

Table IV. A selection of stress inversion results from the present investigation. Data sets *M*4 (magnitudes over 4), WEST, TYR, AEOL and EAST refer to sectors indicated in fig. 7. Data sets ALL, ALL4 and ALL35 include, respectively, all events in the database with focal depth less than 50 km (tables II and III), the same with magnitudes over 4 (ALL4) and over 3.5 (ALL35). *N* and *F* are, respectively, the number of events in the subset and the «average misfit» corresponding to the stress solution.

Set	Depth	N	F	σ_1		σ_2		σ_3		R
				Dip	Strike	Dip	Strike	Dip	Strike	
ALL	2-49	42	11°.5	49	198	27	324	28	70	0.4
*M*4	3-39	13	5°.1	20	180	65	322	14	85	0.2
ALL4	3-39	15	6°.4	45	0	45	186	3	93	0.5
ALL35	2-49	22	9°.0	38	192	37	319	30	75	0.2
WEST	2-39	28	9°.1	49	198	27	324	28	70	0.4
TYR	5-49	17	9°.0	49	198	22	316	32	61	0.3
AEOL	5-39	14	6°.9	64	213	12	328	23	63	0.3
EAST	2-38	19	8°.4	50	198	38	41	11	302	0.6

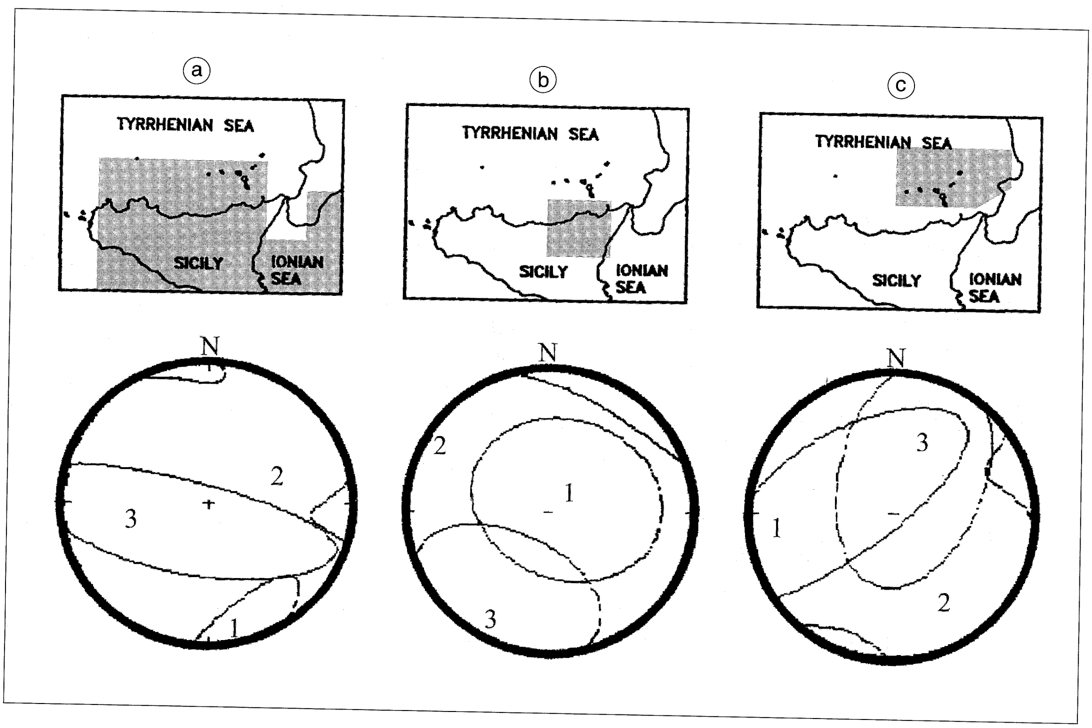

Fig. 5a-c. 90% confidence areas of the maximum (1) and minimum (3) compressive strain orientations for three sub-volumes of the study region. The orientation of the intermediate compressive strain axis (2) is given without confidence limits.

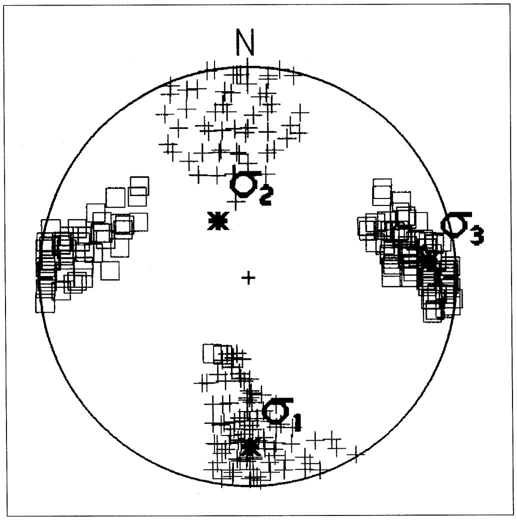

Fig. 6. Lower hemisphere projections of the orientations of the principal stresses obtained for data set *M*4 (table IV and fig. 7). Crosses and squares define the 90% confidence limits of the greatest and least principal stress orientations, respectively.

6. Conclusions

As expected, the analysis of seismicity occurring in the highly heterogeneous lithospheric structure of Sicily and surroundings, performed using a recently proposed 3D velocity model, allowed us to improve the quality of source parameters, compared to standards attained in previous investigations carried out by 1D models. New results concerning earthquake space distribution and focal mechanisms were used for the analysis of seismic stress and strain at different scales in the region. The major findings of previous studies performed in 1D environments (see *e.g.*, Caccamo *et al.*, 1996; Neri *et al.*, 1996) appear to be confirmed and better supported by the present investigation. On a regional scale (earthquake magnitudes over 4) a nearly north-south crustal shortening is evidenced by strain computations in most of Sicily, with the exception of the northeastern corner of the island (Messina Straits area) corresponding to the southern edge of the major Calabrian arc tensional domain. Stress inversion of earthquake

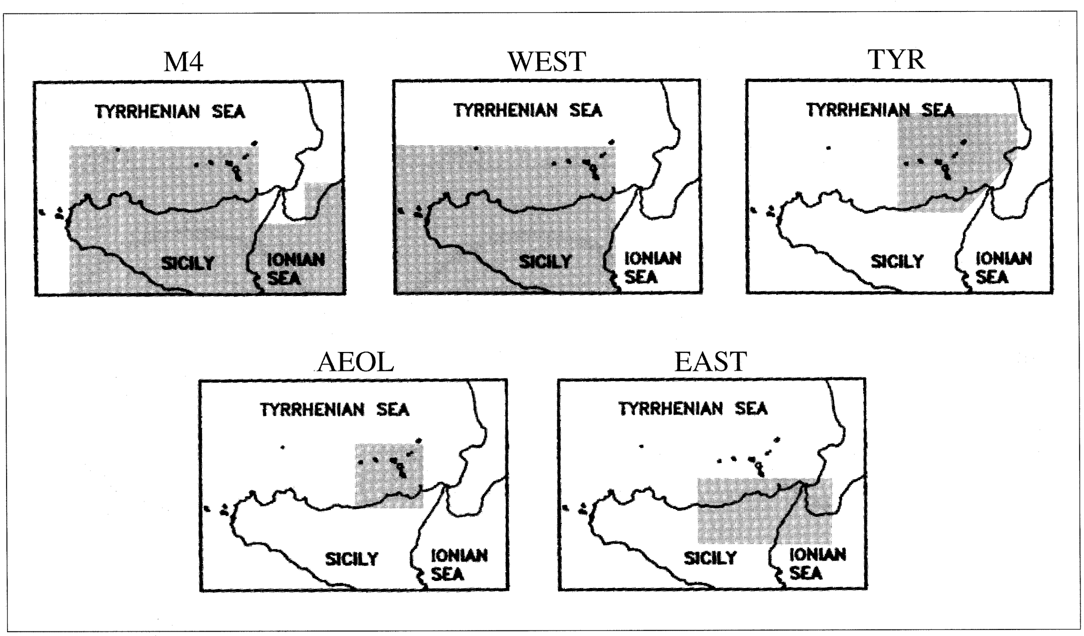

Fig. 7. Sectors relative to several earthquake subsets, as used for stress inversion runs (table IV).

fault-plane solutions led to quite similar results, indicating a low-dip north-south σ_1 in the same area affected by shortening, when the strongest events were considered. These seismic stress and strain results are compatible with geologic information in Central-Western Sicily (Ben-Avraham and Grasso, 1990) and the Calabrian arc (Ghisetti, 1984, 1992; Bousquet *et al.*, 1987), and with structural data from exploration geophysics (Finetti and Del Ben, 1986). Seismic strain releases are clearly larger in the Calabrian arc tensional domain (maximum magnitudes around 7) than in the Sicily compressive domain (around 6). This could be due to different energies associated with the two main tectonic sources which are suspected to act in the Central Mediterranean – Apennines region: the Africa-Europe north-south slow convergence, and the faster eastward roll-back of a westward-dipping Adriatic-Ionic subduction slab (Cinque *et al.*, 1993). When low-magnitude earthquakes, which are more specific markers of local tectonic situations, are used for stress inversion and strain computations, a clear increase is observed in the heterogeneity level, also when limited-extent sub-volumes of the study region are considered. Sub-volumes are often found to display significant differences in deformation style with respect to regional domains, in agreement with the general scheme of stress-strain variable patterns at different scales already proposed in the literature (see *e.g.*, Rebai *et al.*, 1992).

REFERENCES

ALBARELLO, D., M. VITI and E. MANTOVANI (1993): Modellazione numerica del quadro deformativo recente della Sicilia e zone circostanti, in *12th GNGTS-CNR Meeting*, abstract volume.

ALBARELLO, D., E. MANTOVANI and M. VITI (1997): Finite element modelling of the recent-present deformation pattern in the Calabrian arc and surrounding regions, *Ann. Geofis.*, **40** (4), 833-848.

ANDERSON, H. and J. JACKSON (1987): Active tectonics of the Adriatic region, *Geophys. J. R. Astron. Soc.*, **91**, 937-983.

BARBERI, F., P. GASPARINI, F. INNOCENTI and L. VILLARI (1973): Volcanism of the Southern Tyrrhenian Sea and its geodynamic implications, *J. Geophys. Res.*, **78**, 5221-5232.

BEN-AVRAHAM, Z. and M. GRASSO (1990): Collisional zone segmentation in Sicily and surrounding areas in the Central Mediterranean, *Ann. Tectonicae*, **4** (2), 131-139.

BEN-AVRAHAM, Z. and M. GRASSO (1991): Crustal structure variations and transcurrent faulting at the eastern and western margins of the Eastern Mediterranean, *Tectonophysics*, **196**, 269-277.

BOUSQUET, J.C., J.G. CHABELLARD, G. LANZAFAME and H. PHILIP (1987): Place du détroit de Messine dans l'évolution géodynamique récente de l'arc Tyrrhenien, *Le Détroit de Messine, Documents et Travaux, IGAL*, **11**, 15-28.

CACCAMO, D., G. NERI, A. SARAO' and M. WYSS (1996): Estimates of stress directions by inversion of earthquake fault plane solutions in Sicily, *Geophys. J. Int.*, **125**, 857-868.

CALCAGNILE, G. and G.F. PANZA (1981): The main characteristics of the lithosphere-astenosphere system in Italy and surrounding regions, *Pageoph*, **119**, 865-879.

CALCAGNILE, G., F. D'INGEO, P. FARRUGIA and G.F. PANZA (1982): The lithosphere in the Central-Eastern Mediterranean area, *Pageoph*, **120**, 389-406.

CIANCIO, V., M. DOLFIN, D. GILLARD and G. NERI (1997): Orientations of the strain main axes in the lithosphere of Sicily and surroundings as deduced from earthquake data, *Boll. Geofis. Teor. Appl.*, **38** (1-2), 1-12.

CINQUE, A., E. PATACCA, P. SCANDONE and M. TOZZI (1993): Quaternary kinematic evolution of the Southern Appenines. Relationships between surface geological features and deep lithospheric structures, *Ann. Geofis.*, **36** (2), 249-260.

DE LUCA, G., L. FILIPPI, D. CACCAMO, G. NERI and R. SCARPA (1997): Crustal structure and seismicity of Southern Tyrrhenian basin, *Phys. Earth Planet. Int.*, **103**, 117-133.

DZIEWONSKI, A.M., G. EKSTRÖM, J.E. FRANZEN and J.H. WOODHOUSE (1987): Global seismicity of 1978: centroid-moment tensor solutions for 512 earthquakes, *Phys. Earth Planet. Int.*, **46**, 316-342.

DZIEWONSKI, A.M., G. EKSTRÖM, J.H. WOODHOUSE and G. ZWART (1991): Centroid-moment tensor solutions for October-December 1990, *Phys. Earth Planet. Int.*, **68**, 201-214.

FINETTI, I. and A. DEL BEN (1986): Geophysical study of the Tyrrhenian opening, *Boll. Geofis. Teor. Appl.*, **28**, 75-155.

FRAZZETTA, G., G. LANZAFAME and G. VILLARI (1982): Deformazioni e tettonica attiva a Lipari e Vulcano (Eolie), *Mem. Soc. Geol. It.*, **24**, 293-297.

FREPOLI, A., A. AMATO and C. CHIARABBA (1993): Studio di meccanismi focali di alcuni terremoti Italiani recenti, in *Proceedings of the GNGTS-CNR Annual Meeting, Rome*, 217-226.

GASPARINI, C., G. IANNACCONE and R. SCARPA (1985): Fault-plane solutions and seismicity of the Italian peninsula, *Tectonophysics*, **117**, 59-78.

GEPHART, J.W. and W.D. FORSYTH (1984): An improved method for determining the regional stress tensor using earthquake focal mechanism data: applications to the San Fernando earthquake sequence, *J. Geophys. Res.*, **89**, 9305-9320.

GHISETTI, F. (1984): Recent deformations and the seismogenic source in the Messina Strait (Southern Italy), *Tectonophysics*, **109**, 191-208.

GHISETTI, F. (1992): Fault parameters in the Messina Strait (Southern Italy) and relations with the seismogenic source, *Tectonophysics*, **210**, 117-133.

GHISETTI, F. and L. VEZZANI (1982): Different styles of deformation in the Calabrian arc (Southern Italy): implications for a seismotectonic zoning, *Tectonophysics*, **85**, 149-165.

GIARDINI, D., A. DZIEWONSKI, J. WOODHOUSE and E. BOSCHI (1984): Systematic analysis of the seismicity of the Mediterranean region using the centroid-moment tensor method, *Boll. Geofis. Teor. Appl.*, **26** (103), 121-142.

GIARDINI, D., B. PALOMBO and N.A. PINO (1995): Long-period modelling of MEDNET waveforms for the December 13, 1990 Eastern Sicily earthquake, *Ann. Geofis.*, **38** (2), 267-282.

GILLARD, D., M. WYSS and J.S. NAKATA (1992): A seismotectonic model for Western Hawaii based on stress tensor inversion from fault plane solutions, *J. Geophys. Res.*, **97** (B5), 6629-6641.

GILLARD, D., M. WYSS and P. OKUBO (1996): Stress and strain tensor orientations in the south flank of Kilauea, Hawaii, estimated from fault plane solutions, *J. Geophys. Res.*, **101**, 16025-16042.

KIRATZI, A.A. (1994): Active seismic deformation in the Italian peninsula and Sicily, *Ann. Geofis.*, **37** (1), 27-45.

KOSTROV, B. (1974): Seismic moment and energy of earthquakes, and seismic flow of rocks, *Izv. Acad. Sci. USSR Phys. Solid Earth*, **1**, 23-40.

LEE, W.H.K. and J.C. LAHR (1975): HYPO71(revised): a computer program for determining hypocenter, magnitude and first motion pattern of local earthquakes, *U.S. Geol. Sur.*, *Open-file Report*, 75-311.

LOCARDI, E. (1988): The origin of the Apenninic arcs, *Tectonophysics*, **146**, 105-123.

LOCARDI, E. and R. NICOLICH (1988): Geodinamica del Tirreno e dell'Appenino Centro Meridionale: la nuova carta della Moho, *Mem. Soc. Geol. Ital.*, **6**, 121-140.

MANTOVANI, E., D. BABBUCCI, D. ALBARELLO and M. MUCCIARELLI (1990): Deformation pattern in the Central Mediterranean and behaviour of the African/ Adriatic promontory, *Tectonophysics*, **179**, 63-79.

MANTOVANI, E., D. ALBARELLO, C. TAMBURELLI, D. BABBUCCI and M. VITI (1997): Plate convergence, crustal delamination, extrusion tectonics and minimization of shortening work as main controlling factors of the recent Mediterranean deformation pattern, *Ann. Geofis.*, **40** (3), 611-643.

MARTINI, M. and R. SCARPA (1983): Earthquakes in Italy in the last century, in *Proceedings of the «Enrico Fermi» International School of Physics. «Earthquakes: Observation, Theory and Interpretation»*, 479-492.

MICHAEL, A.J. (1987): Use of focal mechanisms to determine stress: a control study, *J. Geophys. Res.*, **92** (B1), 357-368.

MORELLI, C., P. GIESE, R. CASSINIS, B. COLOMBI, I. GUERRA, G. LUONGO, S. SCARASCIA and K.G. SCHUTTE (1975): Crustal structure of Southern Italy. A seismic refraction profile between Puglia-Calabria-Sicily, *Boll. Geofis. Teor. Appl.*, **17**, 182-210.

NERI, G., D. CACCAMO, O. COCINA and A. MONTALTO (1991): Shallow earthquake features in the Southern Tyrrhenian region: geostructural and tectonic implications, *Boll. Geofis. Teor. Appl.*, **33** (129), 47-60.

NERI, G., D. CACCAMO, O. COCINA and A. MONTALTO (1996): Geodynamic implications of recent earthquake data in the Southern Tyrrhenian Sea, *Tectonophysics*, **258**, 233-249..

PARKER, R.L. and M.K. MCNUTT (1980): Statistics for the one-norm misfit measure, *J. Geophys. Res.*, **85**, 4429-4430.

PATACCA, E., R. SARTORI and P. SCANDONE (1990): Tyrrhenian basin and Apenninic arcs: kinematic relations since late Tortonian times, *Mem. Soc. Geol. Ital.*, **45**, 425-451.

PLOMEROVÁ, J., V. BABUŠKA and R. SCARPA (1998): Teleseismic *P*-residual study in the Italian region – inferences on large scale anisotropic structure of the subcrustal lithosphere, *Ann. Geofis.*, **41** (1), 33-48.

POLLITZ, F.F. (1991): Two stage model of African absolute motion during the last 30 millions years, *Tectonophysics*, **194**, 91-106.

REASENBERG, P.A. and D. OPPENHEIMER (1985): FPFIT, FPPLOT AND FPPAGE: fortran computer programs for calculating and displaying earthquake fault-plane solutions, *U.S. Geol. Sur.*, *Open-file Report*, 85-739.

REBAI, S., H. PHILIP and A. TABOADA (1992): Modern tectonic stress field in the Mediterranean region: evidence for variation in stress directions at different scales, *Geophys. J. Int.*, **110**, 106-140.

SCANDONE, P. (1993): Modello sismotettonico d'Italia, in *12th GNGTS-CNR Meeting*, abstract volume.

SCARPA, R. (1982): Travel-time residuals and three-dimensional velocity structure of Italy, *Pageoph*, **120**, 583-606.

SELVAGGI, G. and C. CHIARABBA (1995): Seismicity and *P*-wave velocity image of the Southern Tyrrhenian subduction zone, *Geophys. J. Int.*, **121**, 818-826.

TAMBURELLI, C., E. MANTOVANI, D. ALBARELLO and D. BABBUCCI (1993): Quadro cinematico nell'area Mediterranea Centro-Orientale, in *12th GNGTS-CNR Meeting*, abstract volume.

THURBER, C.H. (1983): Earth structure and earthquake locations in the Coyote Lake area, Central California, *J. Geophys. Res.*, **88**, 8226-8236.

THURBER, C.H. (1993): Local earthquake tomography: velocity and V_p/V_s-theory, in *Seismic Tomography: Theory and Practice*, edited by H.M. IYER and K. HIRAHARA (Reidel, Berlin), 563-583.

WYSS, M., B. LIANG, W.R. TANIGAWA and W. XIAOPING (1992): Comparison of orientations of stress and strain tensor based on fault plane solutions in Kaoiki, Hawaii, *J. Geophys. Res.*, **97** (B4), 4769-4790.